J Mater Sci (2011) 46:3108–3118
DOI 10.1007/s10853-010-5190-0

Quantifying the dispersion of carbon nanotubes in thermoplastic-toughened epoxy polymers

R. D. Brooker · F. J. Guild · A. C. Taylor

Received: 7 October 2010 / Accepted: 13 December 2010 / Published online: 5 February 2011

Abstract The distribution of particles within modern materials must be defined to understand the change in properties attained by their addition. Two methods of analysis, which use different size scales, are presented here. These methods are applied to characterise the dispersion of multi-walled carbon nanotubes in a thermoplastic-toughened epoxy polymer. First, the greyscale method uses transmission optical micrographs, and calculates the ratio of the variance/mean of the greyscale values. Higher values indicate a greater degree of clustering; lower values may be described as showing a 'better' distribution of nanotubes, hence allowing the results to be ranked. This method is relatively easier to carry out, but care must be taken to use a consistent small thickness of sample. Secondly, the quadrat analysis uses transmission electron micrographs of the same materials, after identifying the centre of each nanotube observed. This defines the distribution on the scale of the nanotubes. Peaks in the relationship between the ratio of the variance/mean and cell size are related to microstructural features such as agglomeration. This scale is expected to be related to the scale of microstructural deformation mechanisms which determine global material properties.

Introduction

Carbon nanotubes were first reported by Iijima [1]. They are finite carbon structures consisting of tubes of graphene sheets. Since then much research has been carried out to determine the properties of nanotubes, as reviewed by Xie et al. [2]. This study has shown that carbon nanotubes have excellent mechanical properties, including a high modulus and strength. These properties have led to interest in their use as reinforcement for polymers.

Hence, many tests have been performed to determine the properties of nanotube-reinforced epoxy polymers. Hsiao et al. [3] investigated the effect of adding multiwalled carbon nanotubes (MWNTs) on the shear strength of adhesively bonded single-lap joints. The results showed that the average shear strength of the lap joint specimens increased as the percentage of carbon nanotubes increased, but this was accompanied by a change in the failure locus from interfacial for the control epoxy to substrate failure for the nanotube-modified adhesives. Ganguli et al. [4] recorded an increase in flexural strength through the addition of carbon nanotubes for a tetrafunctional epoxy cured with diaminodiphenyl sulfone (DDS). The addition of 1 wt% MWNT increased the strength from 70 MPa for the control epoxy to 170 MPa. The fracture toughness showed a 3-fold increase when 1 wt% MWNT were added, from 1.3 to 4.0 MPa/m$^{1/2}$. Therefore, it was concluded there was a significant improvement in both the toughness and the ultimate strength of the epoxy.

Improvements in mechanical properties have not been reported by all researchers. Liu and Wagner [5] found no effect on the tensile properties of an amine cured diglycidyl ether of bis-phenol A (DGEBA), with the addition of up to 1 wt% MWNT. Hernández-Pérez et al. [6] investigated the effect of aspect ratio of nanotubes on various properties of nanotube/epoxy composites. They found that the fracture properties, especially, were much improved for nanotubes with high aspect ratios. Nanotubes with low aspect ratios, around 50, gave very little improvement in fracture properties, although they were easier to disperse than the nanotubes with high aspect ratios.

R. D. Brooker · F. J. Guild · A. C. Taylor (✉)
Department of Mechanical Engineering, Imperial College London, South Kensington Campus, London SW7 2AZ, UK
e-mail: a.c.taylor@imperial.ac.uk

This inability to achieve a good dispersion is one of the main problems with using carbon nanotubes, since it appears that the full potential of these materials cannot be realised unless good dispersion is attained. Nanotube-reinforced polymers have been predicted to have excellent properties, but poor dispersion of the nanotubes within the polymer and the presence of entanglements or aggregates is one factor leading to drastic weakening of the nanotube-modified materials [2]. Single-walled nanotubes have a specific problem dispersing since they tend to form rope-like bundles due to the strong van der Waals forces and they have a high surface area, a lack of functional sites and stable chemical characteristics [7]. Song and Youn [8] investigated the effects of dispersion on a variety of properties. They found that dispersion had little effect on the tensile modulus. The tensile strength and elongation at break were increased with an increasing percentage of well-dispersed nanotubes, but with poorly dispersed nanotubes, the tensile strength decreases.

Sonication has been shown to improve the dispersion of carbon nanotubes in epoxy by Lau et al. [9] and Fiedler et al. [10], and of carbon nanofibres by Gershon et al. [11]. Lau et al. found that the nanotubes in the unsonicated mixtures would be agglomerated together with a non-uniform distribution of the nanotubes. Ganguli et al. [4] achieved dispersion using a dual axis centrifugal mixer. When an unnotched fracture surface was examined with a scanning electron microscope (SEM) it was found that the nanotubes were well dispersed and that there was no evidence of agglomeration of nanotubes. Calendering was used by Fiedler et al. [10] along with sonication and stirring. While sonication was found to leave agglomerates, stirring and especially calendering gave good dispersion. Xie et al. [2] suggest that chemical functionalisation is needed to achieve good dispersion. However, Gong et al. [12] found that dispersion was not perfect even when a surfactant was used.

Although the mechanical properties of carbon nanotubes are good, the performance of nanotube-modified epoxies can be poor. Many authors have explained this as a result of poor dispersion. Hence, much study has been undertaken to investigate various methods of dispersion. However, little study has been undertaken on how to quantify the degree of dispersion, which would allow a better comparison of the efficacy of dispersion techniques.

An exception is the recent study by Gershon et al. [11], who measured the modulus of a polymer, of dispersed carbon nanofibres and agglomerated nanofibres using nanoindentation. They then used a rule of mixtures approach to calculate the volume fraction of each phase (i.e. polymer, dispersed particles, agglomerated particles) and compared this with the volume fraction measured using transmission optical microscopy. This article presents methods to quantify the degree of dispersion of carbon nanotubes from micrographs, using a greyscale and a quadrat technique.

Measurement of dispersion

Quadrat method

The method of quadrat analysis dates from geographical methods developed during the Second World War to quantify crop production. The method has been fully described elsewhere [13]. The analysis is applied to a 2-dimensional image of the dispersion with the objects of interest clearly defined, for example via grey scale. The scale of the smallest object of interest is identified and the area is then divided into square cells or quadrats of that scale. Within each quadrat the number of, or the area occupied by, the objects of interest is determined. This data, including the location of each quadrat, is then transferred to a spreadsheet for further analysis.

The variability of the measurements can be expressed as the variance [14]. The variance of the data and the mean value in the measured quadrats is determined. Data for conglomerates of quadrats, described as cells, is then calculated; these cells may be square areas or lines of neighbouring quadrats along orthogonal axes with respect to the dispersion. The variability of variance and mean with cell area or length is thus determined.

For a perfectly random distribution, the mean value is equal to the variance [14]. For each cell size, the ratio of variance to mean is determined. The variability of this ratio from unity describes the non-random or clustered nature of the distribution. The scale of clusters can be identified from the cell size associated with peaks in the graph.

Greyscale analysis

This method of analysis is closely related to the quadrat method. The greyscale of an image and its variability is captured using image analysis software; the variance of the data is calculated. Essentially, this method is identical to quadrat analysis at one single scale, namely the pixel size used, assuming that a 2-dimensional image is measured.

Materials

Constituents

The aim of the analyses is to determine the dispersion of carbon nanotubes within an epoxy matrix. The effect of addition of a further thermoplastic phase is also assessed. The epoxy used was a blend of two amine cured resins:

triglycidyl aminophenol (TGAP), (MY0510) and a diglycidyl ether of bisphenol F (DGEBF), (PY306). Both were manufactured by Huntsman, Switzerland. The curing agent was an amine hardener, 4,4″-methylenebis-(3-chloro 2,6-diethylaniline), (MCDEA) from Lonza, Switzerland, which is in powder form and has an active hydrogen content of 94.85 g/equivalent. The thermoplastic used is from Cytec Engineered Materials, Wilton. It is a poly(ether sulfone) copolymer with reactive endgroups, and is supplied in powder form. The exact structure is confidential, as are many of its properties; however, it is known to have a glass transition temperature between 180 and 190 °C.

Multiwalled carbon nanotubes were sourced from Thomas Swan & Co (Consett); these are chemical vapour deposition formed nanotubes which are not functionalised. These have the product reference P940 and have the following typical properties: average diameter of 10–12 nm; average length of microns; purity of 70–90% [15]. Samples were prepared using either the dry nanotubes, or using the nanotubes dispersed within the thermoplastic at a loading of 1% by weight.

Preparation of blends

The amine cured epoxy system used the constituents in the following ratio, 1 PY306:1.17 MY0510:1.42 MCDEA by weight. The two epoxies were put in a beaker and mixed briefly together using a spatula.

The dry nanotubes were added to the mixed epoxy resins. The nanotubes were stirred in using a spatula, and the beaker was placed in an ultrasonic bath (Grant MXB6) for sonication. The bath was run continuously and the mix was stirred thoroughly each day using a spatula. The nanotubes were sonicated into the epoxy for approximately 120 h.

Samples incorporating the thermoplastic were prepared using both the dry nanotubes dispersed in the epoxy and nanotubes supplied dispersed within the thermoplastic. The dry nanotubes were added as described above by sonicating the nanotubes into the epoxy, before adding the thermoplastic. The thermoplastic powder was added and this was stirred in using the mechanical stirrer at 650 rpm for at least 2 h at 120 °C until all the thermoplastic had dissolved. For the nanotubes supplied dispersed in the thermoplastic, the thermoplastic/nanotube mixture was added to the epoxy and stirred as for the pure thermoplastic.

When 25 wt% thermoplastic was required, the thermoplastic was added in two batches of approximately equal weight, each batch being stirred in for 2 h at 650 rpm and 120 °C. The mix was allowed to cool overnight, re-heated the following day before the MCDEA was added.

The MCDEA was added and the mix was placed in an oven at 120 °C and stirred for 1 h with an overhead stirrer fitted with a radial flow impeller. The unmodified epoxy was stirred at about 200 rpm, and the thermoplastic-modified epoxy at 650 rpm. This ensured that the MCDEA, which was added in powder form, dissolved fully into the epoxy.

Curing of the formulations in situ in the transmission optical microscope showed that the nanotubes are relatively mobile [16]. The nanotubes were found to agglomerate during the cure cycle. The higher the percentage of thermoplastic then the lesser the degree to which the nanotubes agglomerate, and the higher the temperature needs to be before the nanotubes begin agglomerating during curing. It is thought that this is due to the increase in viscosity of the resin with adding thermoplastic. The higher the viscosity then the harder it is for the nanotubes to move through the resin, so the slower they move and the higher the temperature needs to be before the viscosity drops to a level at which the nanotubes can move. The addition of either thermoplastic or nanotubes increased the viscosity. Once the resin reaches the gel point the nanotubes can no longer move, and the current dispersion is frozen. The nanotubes in the resin with higher percentages of thermoplastic begin moving later in the cure cycle (i.e. at a higher temperature), and move more slowly, so it is to be expected that the final dispersion is better.

Preparation of samples

Plates were prepared using picture frame moulds. The mixture was degassed in a vacuum oven before and after pouring into the mould. The plates were cured by heating at 1 °C/min and then held at 180 °C for 5 h. The plates were left to cool to room temperature in the mould. The cured plates were typically 6-mm thick. Samples for mechanical and fracture testing were machined from the plates, as described by Brooker et al. [17].

Resultant morphology

The unmodified epoxy was a homogeneous thermoset. When 15 wt% of the poly(ether sulfone) copolymer was added, the morphology of the thermoplastic/epoxy composites showed an apparently random distribution of equally sized thermoplastic spheres of about 1-μm diameter [16, 17]. However, when the content of thermoplastic was increased to 25 wt%, the morphology becomes co-continuous, with interpenetrating regions of the thermoplastic-rich phase and the epoxy-rich phase. There is also some localised phase-inversion within the thermoplastic-rich phase, which may be observed as spheres of epoxy polymer up to 0.6 μm in diameter in the thermoplastic phase. There are also thermoplastic spheres in the epoxy-rich phase with a diameter of 0.5 μm. The morphology of the thermoplastic appeared

unchanged with the addition of the nanotubes. The nanotubes were mostly dispersed within the epoxy phase rather than within the thermoplastic.

Analysis

The quadrat analysis required the resolution of the individual nanotubes, which was achieved using transmission electron microscopy; magnification of times 80,000 was used. Specimens for transmission electron microscopy (TEM) were prepared using an ultramicrotome at room temperature. Planar sections were cut from the specimens with a diamond knife and were floated on water. Sections with a thickness of about 90 nm were selected and transferred to a copper grid. The transmission electron microscope used was a JEOL 2000FX Mk2, used at 200 kV. Overlapping images, each representing an area of approximately 1.7 μm by 1.3 μm, were taken to allow a montage to be assembled. A typical montage contained around 30 images analysing an area of about 66 μm square. The maximum extent of the montage is limited by the mesh size of the copper grid used to support the sections.

The greyscale analysis does not require the resolution of individual nanotubes; optical microscopy can be used. A transmission optical microscope (Nikon Optiphot II) was used. A planar section of the specimen, approximately 6 mm square, was taken and bonded onto a glass slide with Araldite instant clear. The surface was then polished using a rotary plate polisher, starting with a 6-μm diamond solution, the finest solution used was a 1-μm diamond solution. The samples were then carefully cut off the slides with a hacksaw and bonded with M-bond AE10 from Vishay Measurements Group, polished sides down onto new slides. The samples were then ground down to about 70-μm thickness with a Struers grinder/polisher and polished again. The image was recorded as a greyscale image of size approximately 420×420 pixels. The digital images were imported into Corel Paint Shop Pro or Adobe Photoshop CS5 to analyse the greyscale distribution. The software packages gave identical results.

The range of samples analysed is shown in Table 1. The concentration of thermoplastic was zero, 15 or 25 wt%. Four different concentrations of nanotubes were used without thermoplastic; three different concentrations were used when thermoplastic was present.

Results

Quadrat method

A typical transmission electron microscopy image is shown in Fig. 1. This image is from the sample containing 15 wt% of thermoplastic with 0.178 wt% of nanotubes dispersed in the thermoplastic. A part of a thermoplastic sphere is shown; it is clear that the nanotubes are dispersed within the epoxy even though they were added to the mix dispersed within the thermoplastic. Nanotubes are observed oriented both parallel to and perpendicular to the cutting plane.

The analysis method chosen was to count the number of nanotubes within a quadrat; or strictly the number of sections of nanotube, as a nanotube may extend out of the image volume. This was done manually. The alternative more automatic approach of recording fractional area occupied by nanotubes was not successful since the nanotubes are insufficiently distinct from the epoxy, especially when they are oriented perpendicular to the cutting plane (see Fig. 1). Each nanotube was assigned a nominal centre, and the nanotube was counted if that centre occurred within the quadrat. This process ensured that each nanotube was only counted once. The quadrat size used for the counting varied for each image between 50 and 80 nm square. Observing Fig. 1, it is clear that this quadrat size is

Table 1 Samples analysed

Sample	wt% Thermoplastic	wt% nanotubes	
		Sonicated into epoxy	Dispersed in thermoplastic
0-0.1-S	0	0.1	–
0-0.178-S	0	0.178	–
0-0.336-S	0	0.336	–
0-0.5-S	0	0.5	–
15-0.1-S 15-0.1-D	15	0.1	0.1
15-0.178-S 15-0.178-D	15	0.178	0.178
15-0.336-S	15	0.336	–
25-0.1-S 25-0.1-D	25	0.1	0.1
25-0.178-S 25-0.178-D	25	0.178	0.178
25-0.336-S 25-0.336-D	25	0.336	0.336

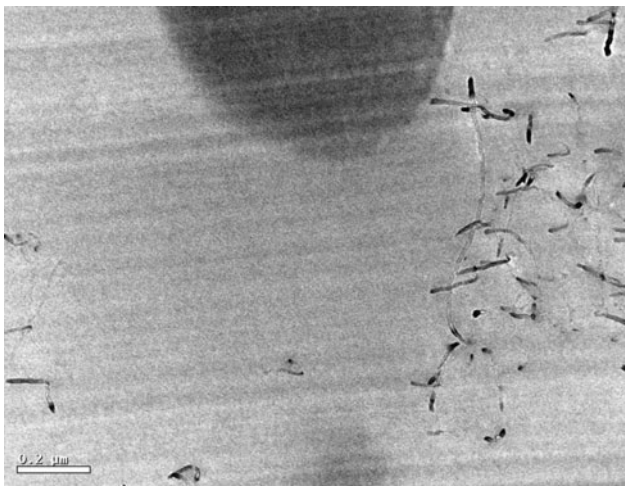

Fig. 1 TEM image showing thermoplastic sphere and carbon nanotubes, for epoxy containing 15 wt% of thermoplastic and 0.178 wt% of carbon nanotubes (15-0.178-D)

at the same scale as the objects of interest. Typical montages used for the counting are shown in Fig. 2; the correct alignment of neighbouring images could only be carried out manually. The acquisition and assembly of the montage was a very time-consuming process; the analysis was carried out for a sufficient range of samples to define the trends but not the full set of samples. Figure 2a is for a 'good' dispersion, while Fig. 2b is for a 'poor' dispersion (see section 'Discussion').

The analysis for larger cell sizes was carried out by increasing the cell size in two orthogonal axes, x and y; these are in-plane directions with respect to the sample so results along these two axes should be in reasonable agreement. The larger cell sizes were analysed either using contiguous cells or overlapping cells. For overlapping cells, the starting quadrat used to form the larger cell is one quadrat beyond the starting quadrat for the previous cell.

Typical results are shown in Fig. 3. The value of the ratio of variance/mean is plotted, the ratio describing the deviation of this value from unity which would occur for a random distribution. The 'cell size' describes the number of quadrats combined in that axis direction; the number of quadrats in the orthogonal direction is always one. The results from Fig. 3a are for overlapping cells; the results in Fig. 3b are for contiguous cells. All results showed an increasing value of the ratio with increasing cell size. Most of the results using contiguous cells showed distinct peaks but most of these peaks disappeared when overlapping cells were used. Such peaks using contiguous cells most probably arose from changing the number of cells analysed as observed previously [18], and hence can be considered to be spurious. In some results distinct peaks were found for overlapping cells; a typical result is shown in Fig. 4. These peaks may be related to a scale of pattern; the cell lengths associated with such peaks are shown in Table 3. Peaks were commonly observed at 600 nm. Further, no peaks were observed at less than 400 nm.

The results for the different materials analysed using overlapping cells are summarised in Table 2. Since different measurement quadrat sizes were used for the different samples, the graphs have been analysed to find the predicted value of variance/mean ratio for cell lengths of 100 and 600 nm. The two orthogonal directions are both

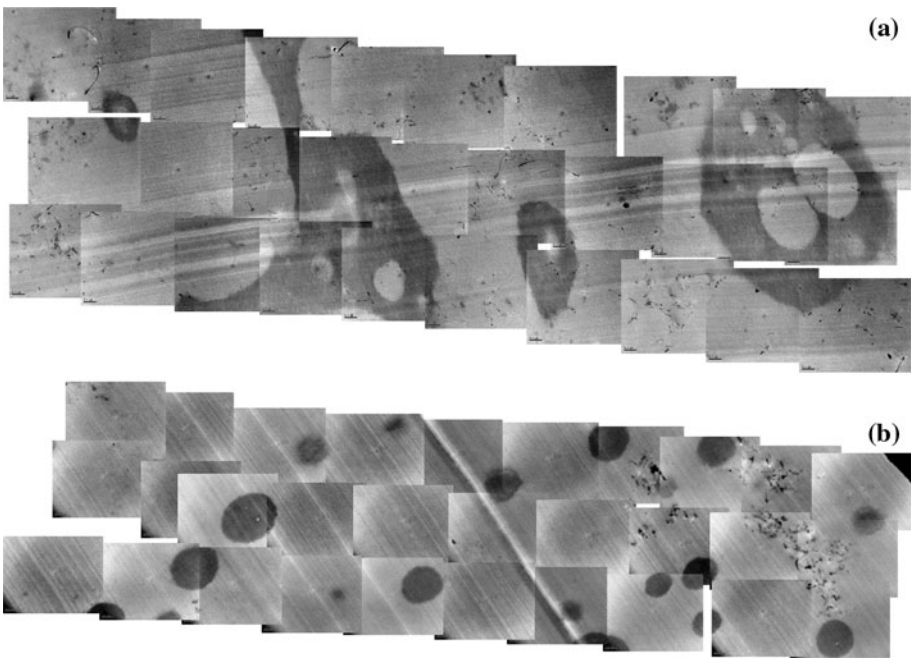

Fig. 2 Typical montages of TEM images for quadrat analysis, for epoxy containing **a** 25 wt% of thermoplastic and 0.336 wt% of carbon nanotubes (25-0.336-D) showing relatively good dispersion, and **b** 15 wt% of thermoplastic and 0.1 wt% of carbon nanotubes showing relatively poor dispersion (15-0.1-S). (*Micron bars* are 0.2-μm long)

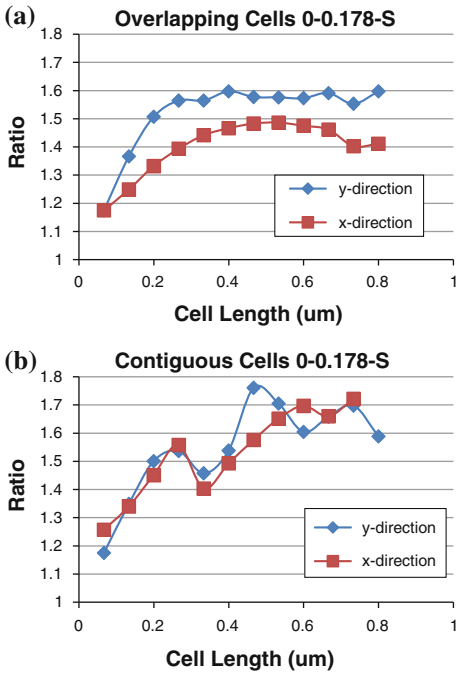

Fig. 3 Typical results from quadrat analysis, for sample 0-0.178-S, using **a** overlapping or **b** contiguous cells

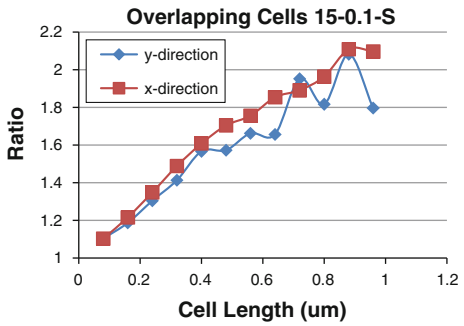

Fig. 4 Typical result from quadrat analysis using overlapping cells showing distinct peaks

in-plane directions with respect to the plate. Results from the two directions are expected to be similar as is shown in Fig. 3b. The results in Table 2 for the two cell lengths are the mean results for the two directions. The values of variance/mean ratio at the two cell lengths have been ordered as 'Rank' describing the values of ratio, rank 1 representing the lowest value of the variance/mean ratio. Note that the rank orders for the two cell lengths are generally approximately equal.

Two example montages are shown in Fig. 2. The montage in Fig. 2a is for the 25-0.336-D sample. Observing the ranking in the quadrat analysis in Table 2 shows that this has a relatively even distribution of nanotubes. The length of several of the clusters of nanotubes appears to be around 400–600 nm; this is discussed in section 'Size of clusters'. Figure 2a shows that the dispersion is relatively 'good', but that clusters are observed on a similar scale to those identified by the quadrat method.

The rank orders for the two cell lengths are generally approximately equal except for the 15-0.1-S material, where there are large differences in the ranks. The ranks are 2 and 7, respectively, at the lengths of 100 and 600 nm. This difference indicates that the degree of dispersion differs considerably at the two lengths used. The good rank at the small length scales shows that the nanotubes are reasonably well dispersed at the small scale, i.e. that they are in loose agglomerates. However, the poor rank at the larger scale indicates that the agglomerates are poorly dispersed. This is confirmed by observation of Fig. 2b, which shows a 'poor' dispersion with a high degree of clustering and significant areas containing no nanotubes.

Greyscale analysis

The greyscale analysis is carried out on the macro-scale using transmission optical microscopy. The images were imported into software which assigned a greyscale to each pixel in the image. The software presented a histogram of the greyscale. The number of pixels of each shade of grey were read off and transferred to a spreadsheet so the mean grey level, standard deviation from that mean and variance could be calculated. Example images and histograms are shown in Fig. 5. The results for the different nanotube-modified materials are summarised in Table 3.

The thickness of the samples analysed was 70 μm, which is much larger than used for the quadrat analysis of 90 nm (0.09 μm). The samples were approximately 6 mm square, and the images were approximately 412 pixels square. Hence, each pixel covers approximately 15 μm square. The nanotubes were supplied with an average diameter of 10–12 nm, and an average length of 5 μm after sonication. Note that sonication does not significantly reduce the length of the nanotubes. The samples were viewed using unfiltered visible (white) light, which covers wavelengths in the range of 390 to 780 nm [19]. The best spatial resolution for a stereo microscope is typically 2 μm [20]. Hence, nanotube agglomerates would be visible, and although individual nanotubes may not be visible due to their small diameter, they will scatter light.

The thermoplastic phase will also scatter light. The spherical particles in the epoxy containing 15 wt% thermoplastic were measured to be approximately 1 μm in diameter, and well dispersed in the epoxy. The epoxy containing 25 wt% of thermoplastic showed a co-continuous morphology, with interpenetrating regions of the thermoplastic-rich phase and the epoxy-rich phase. There was also some localised phase-inversion within the thermoplastic-rich phase, with epoxy spheres up to 0.6 μm in

Table 2 Summary of results from quadrat analysis using overlapping cells

Sample	Quadrat size (nm)	Values of ratio (mean)		Length at peaks (nm)
		Length 100 nm / rank	Length 600 nm / rank	
0-0.1-S	n/d			
0-0.178-S	67 × 67	1.240 / 6	1.524 / 4	500
0-0.336-S	n/d			
0-0.5-S	n/d			
15-0.1-S	80 × 80	1.127 / 2	1.732 / 7	700, 900
15-0.1-D	50 × 50	1.015 / 1	1.226 / 1	400, 600
15-0.178-S	62 × 62	2.809 / 10	5.295 / 9	n/a
15-0.178-D	53 × 53	2.665 / 9	8.745 / 10	600
15-0.336-S	80 × 80	1.287 / 7	1.811 / 8	600
25-0.1-S	n/d			
25-0.1-D	80 × 80	1.192 / 3	1.364 / 2	800
25-0.178-S	57 × 57	1.449 / 8	1.638 / 5	400, 650
25-0.178-D	80 × 80	1.211 / 5	1.700 / 6	600, 800
25-0.336-S	n/d			
25-0.336-D	67 × 67	1.196 / 4	1.487 / 3	700, 900

diameter within the thermoplastic, and some thermoplastic spheres in the epoxy-rich phase with a diameter of 0.5 μm [17]. Greyscale analysis of these control samples, i.e., those without nanotubes, gave a relatively narrow peak in the greyscale distribution. The calculated variances for the unmodified epoxy and the sample with 15% thermoplastic were approximately 5. The 25 wt% thermoplastic sample gave a variance of 11. These values are an order of magnitude, or two orders in some cases, less than the variances measured for the nanotube-modified samples, see Table 3. Thus, it is reasonable to assume that the presence of the thermoplastic has no significant effect on the measured values for the nanotube-modified samples.

The most reliable comparison of results in Table 3 is the ratio of variance/mean value of the grey level. The value of this ratio takes into account any variation in the overall brightness of the image. All values in Table 3 are greater than one, indicating a tendency to cluster at this scale of measurement. Higher values indicate a greater degree of clustering; lower values may be described a showing a 'better' distribution of nanotubes. The results have been ordered as 'Rank' describing the values of ratio, rank 1 representing the lowest value of the variance/mean ratio.

The results in Table 3 and Fig. 6 show that the dispersion is generally the best for the samples with 25% of thermoplastic, while the samples with no thermoplastic show the highest ranking and hence the poorest dispersion. These numerical values are supported by comparing Fig. 5b, d and c, e. An exception to this trend is the 0-0.178-S sample, where the dispersion was so poor that few nanotubes are observed in the image, as they are generally collected at one end of the sample.

In general, the samples where the nanotubes were sonicated into the epoxy show a lower ranking, and hence a better dispersion than those samples made with nanotubes originally dispersed in the thermoplastic. This can be seen from Table 3, or by comparing Fig. 5b, c and d, e.

The greyscale images in Fig. 5 show that the nanotubes are typically present in necklace-like structures. This can give two peaks in the greyscale histograms, one for the nanotube-rich areas and one for the nanotube-poor areas, see Fig. 5c for example.

Discussion

Comparison of methods

The greyscale analysis is essentially the same analysis approach as the quadrat analysis but at a single cell size and at a much larger scale. The results from the quadrat analysis have been compared for two different cell lengths. The cell lengths corresponding to the peaks, using overlapping cells, have been identified (see Table 2). The results from the greyscale analysis are for cell size approximately 15 μm square, i.e., the pixel size, which is about three orders of magnitude larger than the cell sizes for the quadrat analysis. The quadrat analysis uses the position of the centres of the sections of nanotube, without considering the length or the position of the rest of the nanotube.

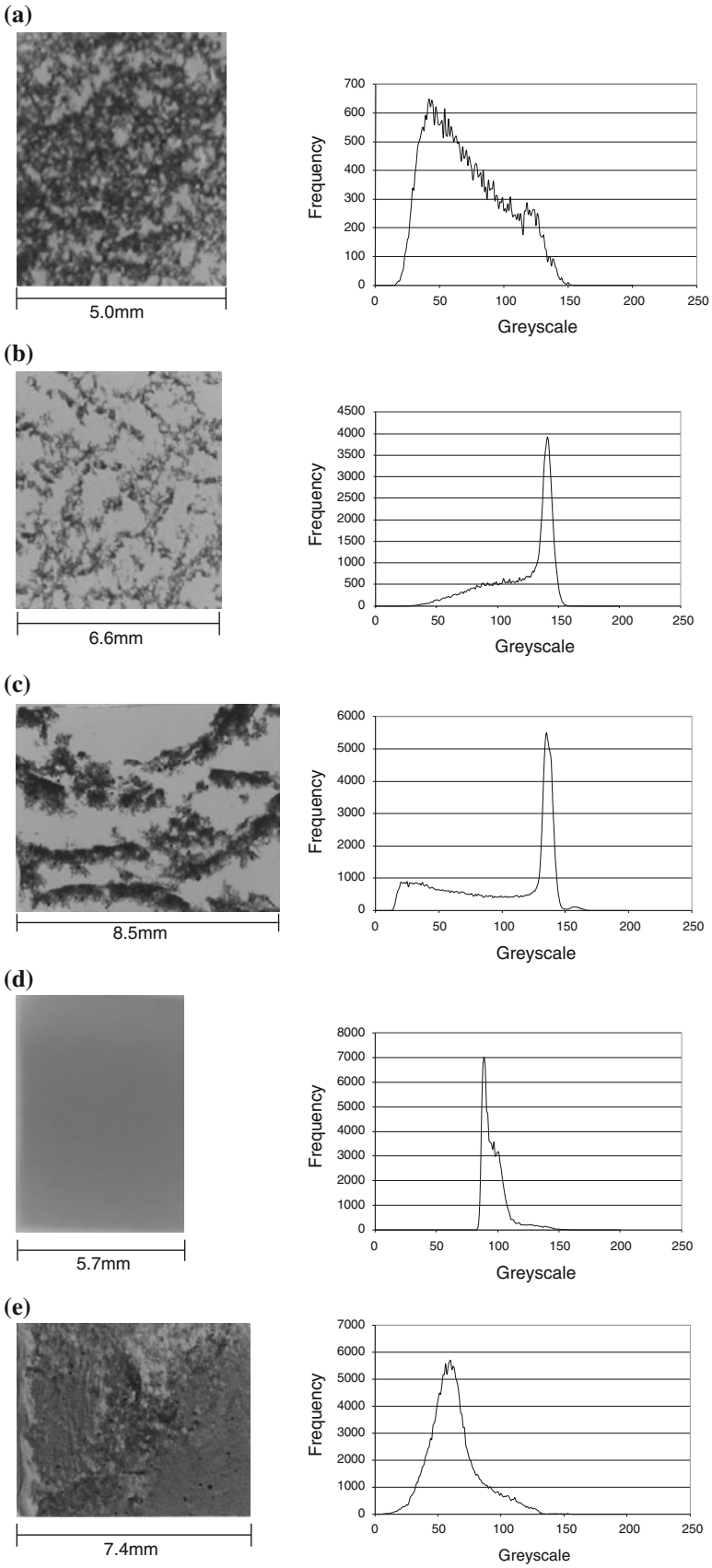

Fig. 5 Greyscale images and corresponding histograms for **a** 0-0.1-S, **b** 15-0.1-S, **c** 15-0.1-D, **d** 25-0.1-S, and **e** 25-0.1-D

Table 3 Summary of results from greyscale analysis

Sample	Standard deviation	Mean	Variance	Ratio / rank
0-0.1-S	29.9	71	894	12.59 / 12
0-0.178-S	17.7	103	313	3.04 / 3
0-0.336-S	29.7	89	882	9.91 / 11
0-0.5-S	31.9	48	1018	21.21 / 15
15-0.1-S	27.2	98	740	7.55 / 7
15-0.1-D	43.4	98	1884	19.22 / 14
15-0.178-S	29.4	94	864	9.19 / 10
15-0.178-D	41.9	107	1756	16.41 / 13
15-0.336-S	20.7	52	428	8.23 / 8
25-0.1-S	10.8	97	117	1.21 / 2
25-0.1-D	20.1	63	404	6.41 / 6
25-0.178-S	8.9	80	79.2	0.99 / 1
25-0.178-D	23.8	102	566	5.55 / 5
25-0.336-S	20.1	82	404	4.93 / 4
25-0.336-D	16.3	32	266	8.31 / 9

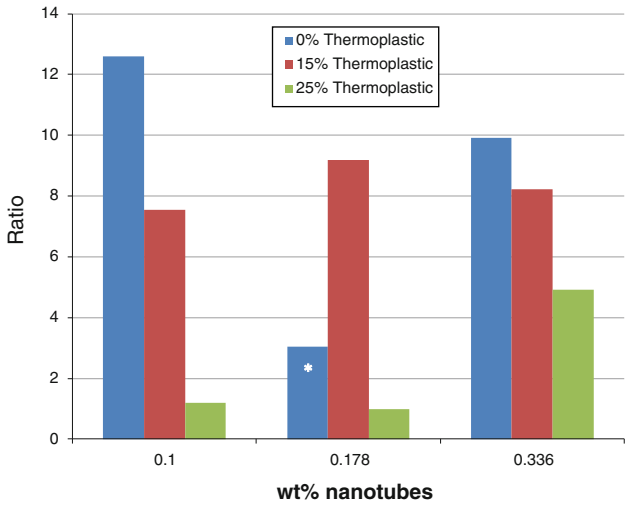

Fig. 6 Ratio of variance/mean versus nanotube content for greyscale analysis of epoxy with 0, 15 and 25 wt% of thermoplastic (*: 0-0.178-S sample shows very poor dispersion at macroscale)

The rankings from both techniques are shown in Tables 2 and 3, but these rankings show significant differences. Inspection of the images in Fig. 5 helps to explain the differences. On the macroscale, as shown by the greyscale images and analysis, the samples are very inhomogeneous, see Fig. 5c for example. Thus there will be large difference in the number and dispersion of nanotubes in different areas of the sample on the microscale, and hence large variations would be expected from quadrat analyses from these different areas. Inspection of the montages used for the quadrat analyses, as shown in Fig. 2, also shows why it is necessary to use a quantitative technique to assess dispersion, and why a relatively large sample size should be used, as there is considerable variation in the dispersion of nanotubes at the nanoscale. This also shows why the use of a single TEM image to characterise the dispersion of nanotubes can be very misleading.

Even for samples that are identified as relatively homogeneous by greyscale analysis, the dispersion measured by the quadrat method can be poor. An example is the 25-0.178-S sample, see Fig. 5d. This shows a rank of 1 by the greyscale method, but of 8 and 5 by the quadrat method at 100 and 600 nm, respectively. Hence, the dispersion at the macroscale is good, but relatively poor at the nanoscale. Thus, it is not sufficient to simply use one of these methods to fully characterise the dispersion of nanotubes.

Comparison of methods of dispersion

The results in Table 3 for the greyscale analysis include five cases where both sonication and dispersion within the thermoplastic has been used to disperse the nanotubes; the pairs of data are highlighted with matching shading in Table 3. For all five cases, lower ratio values are found for the material where sonication into the epoxy has been used. It is concluded that this method reduces the clustering of the nanotubes at this microstructural scale. The results in Table 2 for the quadrat analysis include three cases where both sonication and dispersion within the thermoplastic has been used to disperse the nanotubes; the pairs of data are highlighted with matching shading in Table 2. For the lower cell length of 100 nm lower ratio values are found for the material where dispersion within the thermoplastic has been used for all three cases. The relative ranking at cell length 600 nm is reversed for two sets of data, although it is noted that values of ratio for these sets are not far apart.

These comparisons for the different scales of nanotube dispersion may be explained in terms of the different methods of dispersion. At the larger scale, demonstrated by the results of the greyscale analysis, sonication leads to a more even overall dispersion of the nanotubes within the whole sample. However, at the scale of the nanotubes themselves, demonstrated by the results of the quadrat analysis, dispersion within the thermoplastic reduces the tendency for the nanotubes to attract each other into clusters. Note that all the nanotubes sonicated into the epoxy are observed within the epoxy phase rather than the thermoplastic phase, see Fig. 2b. When the nanotubes were supplied dispersed in the thermoplastic, most of the nanotubes in the cured material are observed within the epoxy phase, although some are present within the thermoplastic, see Fig. 2a.

Addition of thermoplastic

The addition of 25 wt% of thermoplastic leads to some changes in overall morphology of the composite. The effect of thermoplastic addition can be assessed by comparing the results between zero content and 15 or 25 wt% content with the nanotubes dispersed using sonication. For the quadrat analysis (see Table 2), the only comparison that can be made is for samples containing 0.178 wt% of nanotubes (0-0.178-S, 15-0.178-S, and 25-0.178-S). (Note that the 15-0.178-S sample shows very poor dispersion at the macroscale, so the results from this sample should be considered with care.) Comparison of the results clearly shows that the increase in viscosity from addition of 25 wt% compared to 15 wt% of thermoplastic reduces the tendency to cluster.

Three sets of comparisons can be made for the results from the greyscale analysis; the values of ratio are compared in Fig. 6. The increase in viscosity from addition of 15 or 25 wt% of thermoplastic reduces the tendency to cluster. This agrees with the observations from the quadrat analysis. For the lower nanotube contents, the ratio for 25 wt% thermoplastic is much less than the other data, which may indicate that the change in morphology may have an effect on the clustering of the nanotubes.

Addition of nanotubes

The results in Fig. 6 show no clear trends in measured distribution from the greyscale analysis arising from the addition of nanotubes. The results from dispersion within the thermoplastic for the greyscale analysis similarly show no clear trends. The results from the quadrat analysis have been carefully examined, and similarly show no clear trends in distribution with addition of nanotubes. The addition of thermoplastic has a much more significant effect than the concentration of nanotubes at these small weight percentages.

Size of clusters

The quadrat analysis finds distinct peaks which may be attributed to cluster size. Such peaks are distinct, as shown in Fig. 4, or more gradual, as shown in Fig. 3a. The cell length associated with these peaks is quoted in Table 2; many peaks were found at around 600-nm cell length. This length may be associated with the observed length of apparent clusters as seen in the montages in Fig. 2. These clusters are loose agglomerates of nanotubes. The greyscale images in Fig. 5 also show clustering, as the nanotubes are typically present in necklace-like structures tens of microns wide. Hence, clustering is observed at many size scales.

Comparison with mechanical tests

The mechanical properties and fracture performance of the thermoplastic-modified epoxy have been discussed by Brooker et al. [17]. For the unmodified epoxy, a Young's modulus of 2.55 GPa was measured. A 0.2% proof stress of 65.2 MPa and a tensile strength of 44.8 MPa were measured. The measured values of Young's modulus and 0.2% proof stress were unaffected by either the addition of nanotubes or the thermoplastic. The tensile strength showed a steady increase as the content of the thermoplastic copolymer was increased, which confirms that there is good adhesion between the epoxy and the thermoplastic phases, as poor bonding would result in a decrease in the tensile strength.

A fracture toughness of 0.68 $MPa/m^{1/2}$ and a fracture energy of 215 J/m^2 was measured for the unmodified epoxy. For the samples with no nanotubes, the fracture toughness and fracture energy of the formulations were found to increase steadily with increasing thermoplastic content, from a fracture energy of 245 J/m^2 using 15 wt% of poly(ether sulfone) copolymer up to a maximum of 530 J/m^2 for the epoxy with 35 wt% thermoplastic. This increase was not, however, linked to the observed changes in morphology, but simply to the weight percentage of the thermoplastic added to the formulation [17]. The addition of carbon nanotubes gave no significant difference in the measured values compared to those for thermoplastic alone. Further study has shown that it is difficult to toughen this particular epoxy [21, 22], and hence it is not surprising that the addition of nanotubes has little effect.

There was no significant difference in the mechanical and fracture properties whether the nanotubes were sonicated into the epoxy or dispersed in the thermoplastic. The addition of the nanotubes also caused no obvious changes in the morphology of the thermoplastic phase.

Conclusions

The distribution of nanotubes within modern materials must be defined to understand the change in properties attained by their addition. Two methods of analysis have been presented here, which described the dispersion of nanotubes at the macro- and nanoscale. However, care must be taken with the interpretation of the results when dispersion is very poor. The analyses showed that increased thermoplastic content, and hence increased viscosity of the resin, led to a better dispersion.

The greyscale method is relatively easier to carry out, although care must be taken to use a consistent small thickness of sample. The quadrat analysis defines the distribution on the scale of the nanotubes and the results of

this analysis can be related to visual observation of the electron micrographs. This scale is expected to be related to the scale of the microstructural deformation mechanisms which determine global material properties. The development of the experimental techniques required to carry out this analysis, including spatial definition of the position of neighbouring micrographs, may make this analysis method more tractable. Further applications of this method of analysis will lead to proper definition of modern nanofilled materials.

Acknowledgements The authors would like to thank the EPSRC and Cytec Engineered Materials for funding the project, and the Royal Society for the Mercer Award which provided funding for some of the equipment used. The authors would like to thank Prof. S.G. Gilmour (Queen Mary, University of London) for his help with the statistical analysis, also Tsung-Han Hsieh and Huang Ming Chong for their help with some of the microscopy.

References

1. Iijima S (1991) Nature 354:56
2. Xie X-L, Mai Y-W, Zhou X-P (2005) Mater Sci Eng R 49:89
3. Hsiao K-T, Alms J, Advani SG (2003) Nanotechnology 14:791
4. Ganguli S, Bhuyan M, Allie L, Aglan H (2005) J Mater Sci 40:3593. doi:10.1007/s10853-005-2891-x
5. Liu L-Q, Wagner HD (2007) Compos Interfaces 14:285
6. Hernández-Pérez A, Avilés F, May-Pat A, Valadez-González A, Herrera-Franco PJ, Bartolo-Pérez P (2008) Compos Sci Technol 68:1422
7. Wang Z, Liang ZY, Wang B, Zhang C, Kramer L (2004) Composites A 35:1225
8. Song YS, Youn JR (2005) Carbon 43:1378
9. Lau K-T, Shi S-Q, Cheng H-M (2003) Compos Sci Technol 63:1161
10. Fiedler B, Gojny FH, Wichmann MHG, Nolte MCM, Schulte K (2006) Compos Sci Technol 66:3115
11. Gershon A, Cole D, Kota A, Bruck H (2010) J Mater Sci 45:6353. doi:10.1007/s10853-010-4597-y
12. Gong X, Liu J, Baskaran S, Voise RD, Young JS (2000) Chem Mater 12:1049
13. Guild FJ, Summerscales J (1998) In: Summerscales J (ed) Microstructural characterisation of fibre-reinforced composites. Woodhead Publishing, Cambridge
14. Chatfield C (1983) Statistics for technology: a course in applied statistics. CRC Press, Boca Raton
15. Thomas Swan (2006) Technical Data Sheet, Elicarb MW (Dry). Thomas Swan & Co., Consett
16. Brooker RD (2009) PhD Thesis, Imperial College London, London
17. Brooker RD, Kinloch AJ, Taylor AC (2010) J Adhesion 86:726. doi:10.1080/00218464.2010.482415
18. Guild FJ, Silverman BW (1978) J Microsc Oxf 114:131
19. Held G (2009) Introduction to light emitting diode technology and applications. Auerbach Publications, Boca Raton
20. Sawyer LC, Grubb DT, Meyers GF (2008) Polymer microscopy. Springer, New York
21. Masania K (2010) PhD Thesis, Imperial College London, London
22. Hsieh TH, Kinloch AJ, Masania K, Taylor AC, Sprenger S (2010) Polymer 51:6284. doi:10.1016/j.polymer.2010.10.048